

Nonlinear shoaling of directionally spread waves on a beach

T. H. C. Herbers and M. C. Burton

Department of Oceanography, Naval Postgraduate School, Monterey, California

Abstract. The shoaling of directionally spread surface gravity waves on a gently sloping beach with straight and parallel depth contours is examined with weakly dispersive Boussinesq theory. In this second-order theory, energy is transferred from the incident waves to components with both higher and lower frequencies in near-resonant nonlinear triad interactions. Directional spreading of the incident waves causes a weak detuning from resonance that is of the same order as the detuning owing to dispersion. Boussinesq theory predictions of the evolution of a single triad (i.e., two primary wave components shoaling from deep water forcing a secondary wave component) are compared to predictions of dispersive finite depth theory for a typical range of beach slopes, incident wave amplitudes, frequencies, and propagation directions. The dependencies of the predicted secondary wave growth on primary wave incidence angles are in good agreement. Whereas the sum frequency response is insensitive to the (deep water) spreading angle of the primary waves, the difference frequency (infragravity) response is significantly reduced for large spreading angles. A stochastic formulation of Boussinesq wave shoaling evolution equations is derived on the basis of the closure hypothesis that phase coupling between quartets of wave components is weak. In this approximation the second- and third-order statistics of random, directionally spread shoaling waves are described by a coupled set of evolution equations for the frequency alongshore wavenumber spectrum and bispectrum. It is shown that a smooth overlap with solutions of dispersive finite depth theory exists in the limit of small beach slope and weak nonlinearity.

1. Introduction

As ocean surface waves shoal from deep to shallow water, amplitudes increase, wavelengths decrease, and propagation directions refract toward normal incidence to the beach. In addition to these linear propagation effects, nonlinear wave-wave interactions can cause significant transfers of energy to wave components with both higher and lower frequencies. Nonlinear effects on waves in deep water ($\kappa h \gg 1$, where κ is the wavenumber and h is the water depth) and intermediate depths ($\kappa h = O(1)$) are usually evaluated with finite depth theory on the basis of Stokes perturbation expansion for small wave slopes ($a\kappa \ll 1$, where a is the wave amplitude) [e.g., Phillips, 1960; Hasselmann, 1962]. At second order, nonlinear interactions between two primary wave components with frequencies and (vector) wavenumbers (ω_1, \mathbf{k}_1) and (ω_2, \mathbf{k}_2) excite secondary waves with the sum $(\omega_1 + \omega_2, \mathbf{k}_1 + \mathbf{k}_2)$ and difference $(\omega_1 - \omega_2, \mathbf{k}_1 - \mathbf{k}_2)$ frequency and wavenumber. These triad interactions are nonresonant [Phillips, 1960], and the amplitudes of the secondary (“bound”) waves are small compared to the primary wave amplitudes. Observations of bound waves in intermediate depths agree well with predictions of second-order finite depth theory [e.g., Herbers *et al.*, 1992, 1994].

In shallow water ($\kappa h \ll 1$) the secondary wave response is strongly amplified because triad interactions involving two primary wave components propagating in approximately the same direction are near resonant. The solutions of finite depth theory are valid only if the Ursell number, $U_r \equiv a/\kappa^2 h^3$, is small

[Ursell, 1953], and this condition is typically violated on beaches. When the relative mismatch Δ of $(\omega_1 \pm \omega_2, \mathbf{k}_1 \pm \mathbf{k}_2)$ from the gravity wave dispersion relation

$$\Delta_{\pm} \equiv \frac{(\omega_1 \pm \omega_2)^2 - g|\mathbf{k}_1 \pm \mathbf{k}_2| \tanh [|\mathbf{k}_1 \pm \mathbf{k}_2|h]}{(\omega_1 \pm \omega_2)^2}$$

is small, energy is transferred from the primary waves to freely propagating secondary waves until the secondary waves eventually run out of phase with the (slightly off-resonance) quadratic forcing terms in the second-order equations [e.g., Armstrong *et al.*, 1962]. The distance over which this detuning of the interaction takes place depends on the resonance mismatch and is infinite for $\Delta = 0$. In the limit of weak nonlinearity (i.e., $U_r \ll 1$) $O(1)$ energy transfers occur only in pure resonant ($\Delta = 0$) interactions over asymptotically large distances (e.g., quartet interactions [Phillips, 1960; Hasselmann, 1962]), but the nonlinearity of waves shoaling on beaches is typically strong enough to cause large cumulative energy transfers in near-resonant triad interactions over moderate (e.g., $O(10)$ wavelengths) distances [e.g., Freilich and Guza, 1984; Elgar and Guza, 1985a]. A useful approximation is provided by the Boussinesq equations, which are based on the assumption that a/h (nonlinearity) and $(\kappa h)^2$ (dispersion) are small and of the same order (i.e., $U_r = O(1)$). Peregrine [1967] extended the Boussinesq equations to varying depth, and these equations have been used extensively in various forms to describe the nonlinear energy transfers in near-resonant triads of shoaling waves. Freilich and Guza [1984] developed a discrete frequency domain Boussinesq model for unidirectional waves propagating over a bottom varying slowly in one dimension that accurately predicts the transformation of wave frequency spectra observed on natural beaches [Freilich and Guza, 1984; Elgar

This paper is not subject to U.S. copyright. Published in 1997 by the American Geophysical Union.

Paper number 97JC01581.

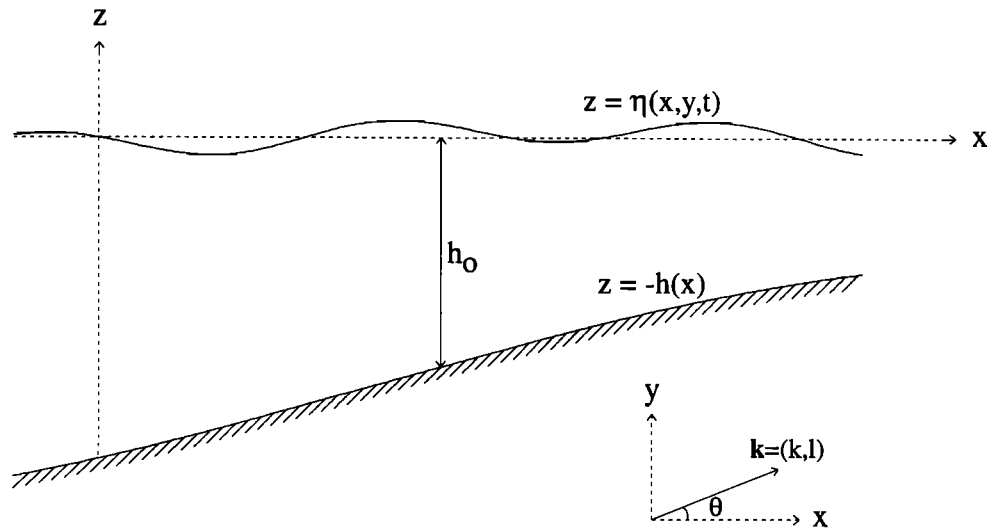


Figure 1. Definitional sketch of variables and coordinate frame. Directionally spread waves propagate over a beach with straight and parallel depth contours. The variable θ denotes the wave propagation direction; \mathbf{k} is the wavenumber vector; and h_0 is a representative water depth of the shoaling region.

and Guza, 1985a]. Liu *et al.* [1985] developed a parabolic approximation to Peregrine's equations, allowing for small directional spreading angles on a two-dimensional beach, but applications to a frequency directional spectrum of waves have not been reported. Recently, Wei *et al.* [1995] introduced a fully nonlinear variant of the Boussinesq equations to simulate the strong nonlinearity in nearly breaking waves.

Whereas fully dispersive finite depth theory solutions are singular at the shoreline, weakly dispersive Boussinesq theory breaks down in intermediate depths ($\kappa h = O(1)$). Various alternative forms of the Boussinesq equations have been derived with improved dispersion relations [Madsen *et al.*, 1991; Nwogu, 1993; Chen and Liu, 1995; Kaihatu and Kirby, 1995]. Although linear propagation effects are accurately incorporated, these extended Boussinesq models do not predict the large deviations from the linear dispersion relation and associated vertical structure of secondary waves in intermediate depths [Herbers and Guza, 1994, and references therein]. The accuracy of second-order nonlinear wave properties predicted by finite depth and Boussinesq theories in the transition region from intermediate depths to shallow water is not well established.

Boussinesq models are often cast in the form of coupled discrete mode equations [Freilich and Guza, 1984] that are cumbersome when applied to continuous spectra of natural wind-generated waves. Recently, stochastic formulations of shallow water wave models were introduced that predict the evolution of wave spectra on the basis of an energy balance equation, analogous to spectral models used in deep water applications [e.g., *The Wave Model Development and Implementation (WAMDI) Group*, 1988]. Abreu *et al.* [1992] developed a model for the nonlinear evolution of the frequency directional wave spectrum based on an asymptotic closure for nondispersive waves by Newell and Aucoin [1971]. In this model, only exact resonances are considered, and non-Gaussian phase coupling between wave triads is neglected. Eldeberky and Battjes [1995] developed a similar model based on the Boussinesq equations that is more appropriate for sloping beaches where the interaction distances are typically short.

In this model (for unidirectional waves) a simple parameterization of phase coupling in near-resonant wave triads is included in the energy balance equation.

In this study, Boussinesq theory is used to investigate sum and difference interactions of directionally spread waves propagating over a beach with straight and parallel depth contours. Predictions of the interactions of a pair of wave components shoaling from deep water (section 2) show that the sum frequency response is insensitive to the incident wave directions but the difference frequency response is significantly reduced for large spreading angles, in good agreement with the properties of second-order bound waves predicted by dispersive finite depth theory. A stochastic formulation of Boussinesq shoaling theory is presented in section 3. A coupled set of evolution equations for the frequency alongshore wavenumber spectrum and bispectrum is derived on the basis of a third-order closure hypothesis (section 4). It is shown that in the limit of small beach slope and weak nonlinearity the spectrum and bispectrum solutions asymptotically match finite depth theory solutions. The results are summarized in section 5.

2. Directional Spreading Effects on Shoaling Waves

Boussinesq equations for weakly nonlinear, weakly dispersive waves [Peregrine, 1967] are used here to describe the propagation of a directionally spread wave field over a beach with straight and parallel depth contours (Figure 1). Even waves with a large oblique incidence angle θ_0 relative to the shore-normal x axis in deep water will refract over a seabed with straight and parallel depth contours so that the angle θ in shallow water is small. In the shallow water limit, Snell's law yields

$$\theta = \kappa h \sin \theta_0 \quad (1)$$

Hence the spreading angles $\Delta\theta$ between wave components arriving from deep water are reduced to $O(\kappa h)$ in shallow water. Herbers *et al.* [1992] show that these small spreading

angles cause a weak detuning of nonlinear triad interactions from resonance that is formally of the same order as the detuning effect of weak dispersion. Secondary waves forced by any pair of obliquely propagating incident waves (even waves arriving at grazing angles from opposite quadrants) nearly obey the linear dispersion relation in shallow water (the mismatch is $O(\kappa h)^2$), and thus a directionally spread shoaling wave field can be described as a spectrum of free waves that are coupled through near-resonant triad interactions.

Assuming a gentle bottom slope $h_x = O(a\kappa)$, the shoaling evolution can be evaluated with standard WKB methods [e.g., *Freilich and Guza*, 1984; *Kirby*, 1990]. The surface elevation function η is expressed as a linear superposition of nearly plane, shoreward propagating waves

$$\eta(x, y, t) = \sum_{p=-\infty}^{\infty} \sum_{q=-\infty}^{\infty} \frac{1}{2} a_{p,q}(x) \exp \{i[\psi_{p,q}(x) + l_q y - \omega_p t]\} \quad (2)$$

where $\omega_p = p\Delta\omega$ and $l_q = q\Delta l$ are the frequency and alongshore wavenumber (with $\Delta\omega$ and Δl the separation of adjacent bands in the Fourier representation), and the amplitude $a_{p,q}$ is a slow function of x owing to the combined effects of shoaling and nonlinear interactions. The evolution equations for the amplitudes $a_{p,q}$ and phases $\psi_{p,q}$ are derived in Appendix A (equations (A9) and (A13)). In dimensional form:

$$\frac{da_{p,q}}{dx} = -\frac{h_x}{4h} a_{p,q} + \frac{3\omega_p}{8g^{1/2}h^{3/2}} \cdot \sum_{m=-\infty}^{\infty} \sum_{n=-\infty}^{\infty} a_{m,n} a_{p-m,q-n} \sin(\psi_{m,n} + \psi_{p-m,q-n} - \psi_{p,q}) \quad (3a)$$

$$\frac{d\psi_{p,q}}{dx} = \frac{\omega_p}{(gh)^{1/2}} + \frac{h^{1/2}\omega_p^3}{6g^{3/2}} - \frac{(gh)^{1/2}l_q^2}{2\omega_p} - \frac{3\omega_p}{8g^{1/2}h^{3/2}a_{p,q}} \cdot \sum_{m=-\infty}^{\infty} \sum_{n=-\infty}^{\infty} a_{m,n} a_{p-m,q-n} \cos(\psi_{m,n} + \psi_{p-m,q-n} - \psi_{p,q}) \quad (3b)$$

The first term on the right-hand side of (3a) is the amplitude growth of the mode due to shoaling (Green's law). The first term on the right-hand side of (3b) is the shallow water wavenumber, and the second term represents phase changes owing to dispersion. Directional spreading contributes phase changes (the third term on the right-hand side of (3b)) that are of the same order as the phase changes owing to dispersion (see Appendix A for the scaling details). The double summation terms contain the amplitude growth and phase changes of a mode resulting from nonlinear interactions of all possible triads in which the mode participates. For unidirectional, normally incident ($l = 0$) waves, (3a) and (3b) reduce to *Freilich and Guza's* [1984, equations (16a) and (16b)] "consistent shoaling model."

The amplitude and phase evolution equations (3a) and (3b) were integrated over a plane beach for the simple case of a single triad interaction in which two primary wave components incident from deep water drive a secondary wave component in shallow water. Although interactions with other wave components are neglected, the "single-scattering" approach is useful to examine the dependence of nonlinear energy transfers on directional spreading angles. The Boussinesq results are compared to second-order bound waves predicted by dispersive

finite depth theory. Similar comparisons were reported by *Madsen and Sørensen* [1993] (unidirectional waves in uniform depth), *Agnon et al.* [1993] (unidirectional waves propagating over a sloping bottom), and *Nwogu* [1994] (directionally spread waves in uniform depth).

For three wave components with frequencies ($\omega^{(1)}$, $\omega^{(2)}$, and $\omega^{(3)}$, all > 0) and alongshore wavenumbers ($l^{(1)}$, $l^{(2)}$, and $l^{(3)}$) that satisfy the triad interaction rules

$$\omega^{(3)} = \omega^{(1)} + \omega^{(2)} \quad (4a)$$

$$l^{(3)} = l^{(1)} + l^{(2)} \quad (4b)$$

the evolution equations (equations (3a) and (3b)) for the amplitudes ($a^{(1)}$, $a^{(2)}$, and $a^{(3)}$) and phases ($\psi^{(1)}$, $\psi^{(2)}$, and $\psi^{(3)}$) reduce to

$$\frac{da^{(1)}}{dx} = -\frac{h_x}{4h} a^{(1)} - \frac{3\omega^{(1)}}{4h^{3/2}g^{1/2}} a^{(2)}a^{(3)} \sin \Phi \quad (5a)$$

$$\frac{da^{(2)}}{dx} = -\frac{h_x}{4h} a^{(2)} - \frac{3\omega^{(2)}}{4h^{3/2}g^{1/2}} a^{(1)}a^{(3)} \sin \Phi \quad (5b)$$

$$\frac{da^{(3)}}{dx} = -\frac{h_x}{4h} a^{(3)} + \frac{3\omega^{(3)}}{4h^{3/2}g^{1/2}} a^{(1)}a^{(2)} \sin \Phi \quad (5c)$$

$$\frac{d\Phi}{dx} = -\frac{h^{1/2}\omega^{(1)}\omega^{(2)}\omega^{(3)}}{2g^{3/2}} - \frac{(gh)^{1/2}(\omega^{(1)}l^{(2)} - \omega^{(2)}l^{(1)})^2}{2\omega^{(1)}\omega^{(2)}\omega^{(3)}} - \frac{3(\omega^{(1)}a^{(2)}a^{(3)2} + \omega^{(2)}a^{(1)}a^{(3)2} - \omega^{(3)}a^{(1)}a^{(2)2})}{4h^{3/2}g^{1/2}a^{(1)}a^{(2)}a^{(3)}} \cos \Phi \quad (5d)$$

where $\Phi = \psi^{(1)} + \psi^{(2)} - \psi^{(3)}$ is the biphas of the triad. In uniform depth ($h_x = 0$), (5a)–(5d) have steady solutions with biphas values $\Phi = 0$ or 180° (i.e., symmetric wave profiles). In the limit of small wave amplitudes these steady Boussinesq theory solutions match exactly the second-order bound waves predicted by finite depth theory in the shallow water limit:

$$a^{(1)} = -D(\omega^{(2)}, l^{(2)}, -\omega^{(3)}, -l^{(3)})a^{(2)}a^{(3)} \quad \Phi = 180^\circ \quad (6a)$$

$$a^{(2)} = -D(\omega^{(1)}, l^{(1)}, -\omega^{(3)}, -l^{(3)})a^{(1)}a^{(3)} \quad \Phi = 180^\circ \quad (6b)$$

$$a^{(3)} = D(\omega^{(1)}, l^{(1)}, \omega^{(2)}, l^{(2)})a^{(1)}a^{(2)} \quad \Phi = 0 \quad (6c)$$

with the coupling coefficient D given by (B8) in Appendix B. Hence a smooth overlap region between the predictions of finite depth and Boussinesq theories is expected for small-amplitude waves propagating over a gently sloping beach. This result is consistent with the smooth overlap of small-amplitude Stokes and Cnoidal waves in shallow water [e.g., *Flick et al.*, 1981].

Equations (5a)–(5d) were used to predict both sum interactions (i.e., component (3) is a secondary wave) and difference interactions (i.e., component (3) is a primary wave) for a range of commonly observed beach slopes and incident swell amplitudes, frequencies, and propagation directions. These Boussinesq results are compared in Figures 2–6 to predictions of finite depth theory in the depth range 10–4 m that approximately spans the transition region from nonresonant to resonant triad interactions. In finite depth theory [e.g., *Hasselmann*, 1962], primary wave components propagating over a gently sloping seabed obey the linear shoaling and refraction relations, and the associated nonresonantly forced secondary waves are completely specified by the local primary wave field (Appendix B). The Boussinesq evolution equations (5a)–(5d)

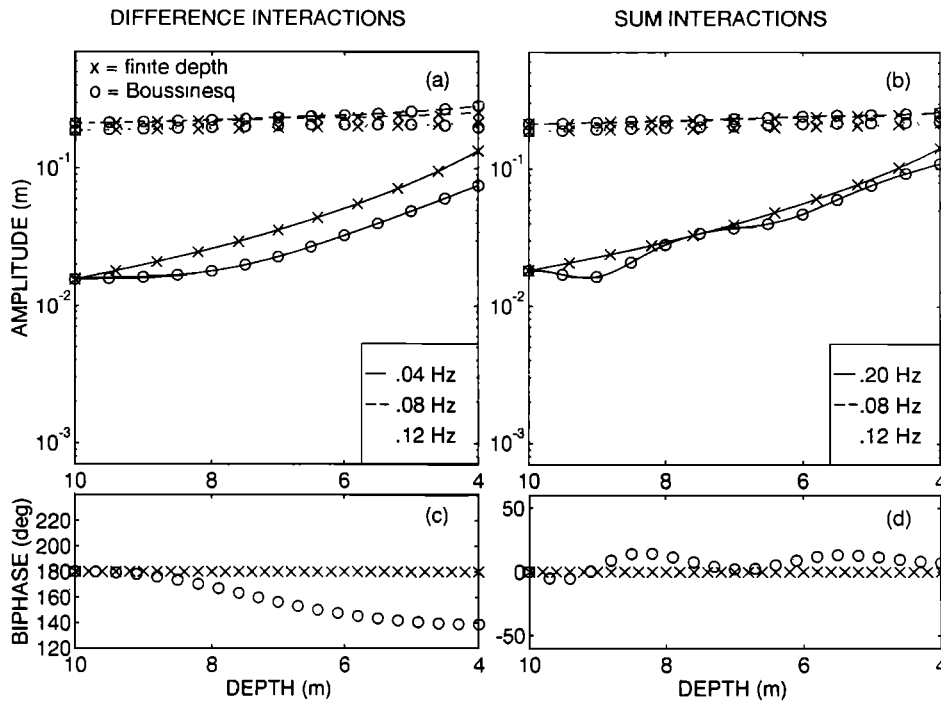


Figure 2. Comparisons of Boussinesq and finite depth theory predictions of the shoaling evolution of a single wave triad. A pair of normally incident wave components with frequencies 0.08 and 0.12 Hz excite a difference frequency (0.04 Hz) secondary wave (Figures 2a and 2c) and a sum frequency (0.20 Hz) secondary wave (Figures 2b and 2d). Figures 2a and 2b show the evolution of the wave amplitudes, and Figures 2c and 2d show the evolution of the biphase.

for the wave amplitudes and biphase were initialized in 10 m depth with the local finite depth theory values ($\Phi = 0$ for sum interactions and $\Phi = 180^\circ$ for difference interactions) and subsequently integrated from 10 to 4 m depth with a first-order finite difference scheme.

Boussinesq and finite depth theory predictions of sum and difference frequency waves forced by a pair of swell components with frequencies 0.08 and 0.12 Hz shoaling on a slope 0.01 beach are compared in Figures 2 and 3. The deep water incident wave amplitudes in these simulations are 0.2 m. The 0.08 Hz component is normally incident in both cases while the 0.12 Hz component is normally incident in Figure 2 and obliquely incident (60° in deep water) in Figure 3. In these simulations, measures of nonlinearity a/h and dispersion κh evolve from initial values of about 0.03 and 0.7, respectively, in 10 m depth ($U_r \approx 0.06$) to ~ 0.1 and 0.4 in 4 m depth ($U_r \approx 0.6$). The growth of the secondary wave in the Boussinesq predictions is controlled by the biphase Φ (equations (5a)–(5c)) and vanishes when Φ is equal to the finite depth theory values of 0 or 180° , as is the case at the initial conditions in 10 m depth. However, the predicted Boussinesq biphases evolve (equation (5d)) and vary between about -5° and 15° for sum interactions (Figures 2d and 3d) and 140° and 200° for difference interactions (Figures 2c and 3c). These deviations from the finite depth theory value cause a gradual evolution of the secondary wave amplitude as the water depth decreases. The evolution of biphases to values close to 90° observed by Elgar and Guza [1985b] and many others occurs in depths shallower than the 10–4 m range of the present computations.

Although in these simulations with finite wave amplitudes and bottom slope the Boussinesq and finite depth theory predictions do not overlap smoothly (e.g., note the initial oscilla-

tions in the Boussinesq amplitude and biphase predictions in Figures 2 and 3), the theories predict comparable secondary wave amplitude growth between 10 and 4 m depth (Figures 2a, 2b, 3a, 3b, and other cases not shown). While the predicted sum frequency secondary wave amplitudes are only slightly smaller for obliquely propagating primary waves than for normally incident primary waves (compare Figures 2b and 3b), the difference frequency secondary wave amplitudes are significantly reduced for large spreading angles (compare Figures 2a and 3a). The directional dependence of the secondary wave response in 4 m depth is further illustrated in Figures 4–6 for a range of beach slopes, incident wave frequencies, and amplitudes with predictions of the normalized secondary wave amplitude a_N defined as the ratio between the secondary wave amplitude and the product of the local primary wave amplitudes. In finite depth theory, a_N is equal to $|D|$ (equation (6) and Appendix B) and thus can be interpreted as a relative secondary wave response for a particular combination of primary wave frequencies and incidence angles that is independent of the primary wave amplitudes. The directional dependencies predicted by Boussinesq and finite depth theories are generally in good agreement. In all cases, sum interactions are insensitive to the deep water spreading angle with approximately a 10–20% decrease in a_N as the spreading angle increases from 0 to 60° , qualitatively consistent with recent numerical [Kaihatu and Kirby, 1992] and laboratory [Elgar et al., 1993] investigations. The sum frequency a_N predicted by finite depth theory are consistently somewhat larger than the Boussinesq predictions, and these discrepancies increase with increasing incident wave amplitudes (about 10–20% and 30–50% for 0.1 and 0.4 m, respectively, Figures 5b and 5d). These differences are likely caused by errors in finite depth theory

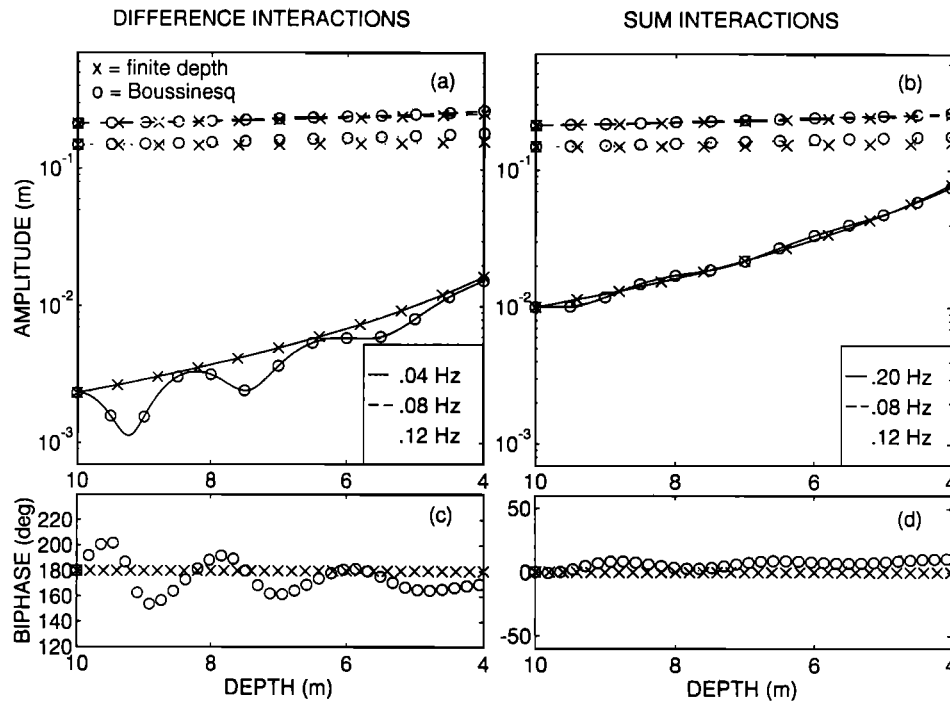


Figure 3. Same comparisons as shown in Figure 2 but with an obliquely propagating (deep water incidence angle 60°) 0.12 Hz wave component.

which overpredicts the secondary wave response for large-amplitude waves (i.e., the predicted secondary wave amplitude is comparable to the primary wave amplitudes in Figure 5d). The smaller a_N predicted by Boussinesq theory (with energy-conserving interactions, equations (5a)–(5c)) for a pair of 0.4 m amplitude incident waves ($U_r \approx 1.2$) is virtually independent of the spreading angle (Figure 5d).

The difference frequency secondary wave response is much more sensitive to the directional spreading angle than the sum frequency response (compare Figures 4a, 4c, 5a, 5c, 6a, and 6c to Figures 4b, 4d, 5b, 5d, 6b, and 6d). Both Boussinesq and finite depth theories predict a strong reduction of a_N (about an order of magnitude) with an increase in deep water spreading angle from 0 to 60° , but large discrepancies between the predictions are noted for runs involving a low difference frequency (0.02 Hz in Figure 4a) or a steep beach (slope 0.03 in Figure 6c). In these cases, where the depth changes from 10 to 4 m over a distance comparable to the secondary wavelength, both theories (based on a slowly varying depth assumption) may have significant errors.

3. Stochastic Shoaling Evolution Equations

Predictions of the shoaling evolution of random, directionally spread waves propagating over a beach with straight and parallel depth contours can, in principle, be obtained by integrating the coupled discrete mode equations (3a) and (3b) for a large number of modes initialized with random amplitudes and phases at the offshore boundary and subsequently averaging the results of many realizations to obtain spectral statistics. This procedure was used successfully by *Freilich and Guza* [1984] and *Elgar and Guza* [1985a] to predict the evolution of one-dimensional (frequency) spectra (i.e., neglecting directional spreading effects) on natural beaches. However, the extension of this approach to two dimensions is far from

straightforward owing to the large number of modes required to simulate continuous frequency directional wave spectra (M. H. Freilich, personal communication, 1989). Furthermore, the detailed specification of amplitudes and phases at the seaward boundary of the computational domain poses a problem in two dimensions since conventional measurements of incident wave conditions on beaches usually provide only certain bulk integral properties of the frequency directional wave spectrum. Here an alternative stochastic formulation of Boussinesq shoaling evolution equations is derived that describes directly the shoaling transformation of continuous spectra of random waves.

The surface elevation function $\eta(x, y, t)$ of random, directionally spread waves propagating over a gently sloping beach with straight and parallel depth contours ($h = h(x)$) can be expressed as

$$\eta(x, y, t) = \sum_{p=-\infty}^{\infty} \sum_{q=-\infty}^{\infty} A_{p,q}(x) \exp [i(l_q y - \omega_p t)] \quad (7)$$

where the complex function $A_{p,q}(x)$ incorporates both the amplitude $a_{p,q}(x)$ and phase $\psi_{p,q}(x)$ of component p, q (equation (2))

$$A_{p,q} = \frac{1}{2} a_{p,q} \exp (i\psi_{p,q}) \quad (8)$$

and Fourier-Stieltjes integrals are approximated by discrete sums to simplify the algebra. The lowest-order statistics of η are described by the variance spectrum

$$E_{p,q} \equiv \mathbf{E}\{A_{p,q}A_{-p,-q}\} \quad (9)$$

where $\mathbf{E}\{ \}$ indicates the expected value. An evolution equation for E can be derived by taking the x derivative of (9)

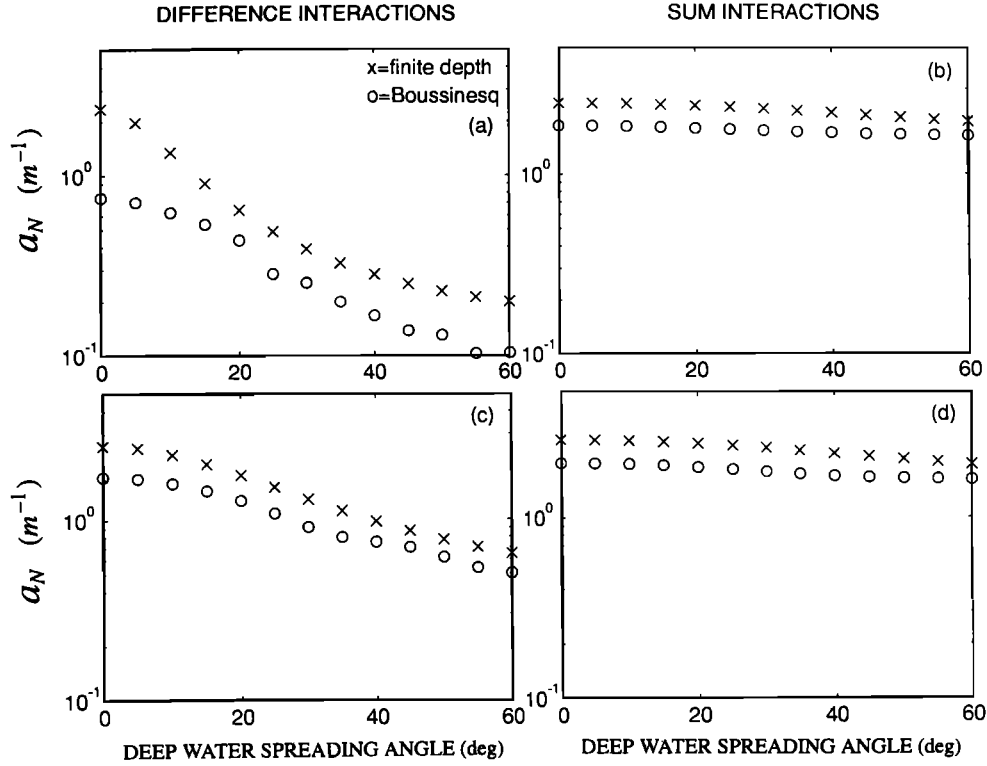


Figure 4. Boussinesq and finite depth theory predictions of the normalized secondary wave amplitude a_N in 4 m depth versus the deep water directional spreading angle of the two primary wave components. The primary wave frequencies are 0.09 and 0.11 Hz (Figures 4a and 4b) and 0.07 and 0.13 Hz (Figures 4c and 4d). The lower-frequency primary component is normally incident, while the deep water incidence angle of the higher-frequency primary component varies between 0 and 60°. Difference and sum interactions are shown in the Figures 4a and 4c and Figures 4b and 4d, respectively. The beach slope is 0.01, and the deep water amplitudes of both primary waves are 0.2 m.

$$\frac{dE_{p,q}}{dx} = \mathbf{E} \left\{ \frac{dA_{p,q}}{dx} A_{-p,-q} \right\} + \mathbf{E} \left\{ A_{p,q} \frac{dA_{-p,-q}}{dx} \right\} \quad (10)$$

In the Boussinesq approximation, $dA_{p,q}/dx$ follows from (8), (3a), and (3b)

$$\begin{aligned} \frac{dA_{p,q}}{dx} = & \left\{ -\frac{h_x}{4h} + i \left[\frac{\omega_p}{(gh)^{1/2}} + \frac{h^{1/2}\omega_p^3}{6g^{3/2}} - \frac{(gh)^{1/2}l_q^2}{2\omega_p} \right] \right\} A_{p,q} \\ & - i \frac{3\omega_p}{4h^{3/2}g^{1/2}} \sum_{m=-\infty}^{\infty} \sum_{n=-\infty}^{\infty} A_{m,n} A_{p-m,q-n} \end{aligned} \quad (11)$$

Substitution of (11) into (10) yields

$$\begin{aligned} \frac{dE_{p,q}}{dx} = & -\frac{h_x}{2h} E_{p,q} - i \frac{3\omega_p}{4h^{3/2}g^{1/2}} \\ & \cdot \sum_{m=-\infty}^{\infty} \sum_{n=-\infty}^{\infty} [\mathbf{E}\{A_{m,n}A_{p-m,q-n}A_{-p,-q}\} \\ & - \mathbf{E}\{A_{m,n}A_{-p-m,-q-n}A_{p,q}\}] \end{aligned} \quad (12)$$

If Gaussian statistics are assumed (i.e., the cubic terms are neglected), then (12) reduces to Green's law for linear shoaling waves in shallow water. Nonlinear triad interactions cause phase coupling between any three wave components obeying the interaction rules (4a) and (4b) (including all cubic terms in (12)), and thus higher-order statistics are needed to describe

nonlinear shoaling waves. The deviations from normality owing to phase-coupled wave triads are uniquely specified by the bispectrum B [Hasselmann *et al.*, 1963]

$$B_{m,n,p-m,q-n} \equiv \mathbf{E}\{A_{m,n}A_{p-m,q-n}A_{-p,-q}\} \quad (13)$$

With this definition the spectrum evolution equation (12) can be expressed compactly as

$$\frac{dE_{p,q}}{dx} = -\frac{h_x}{2h} E_{p,q} + \frac{3\omega_p}{2h^{3/2}g^{1/2}} \sum_{m=-\infty}^{\infty} \sum_{n=-\infty}^{\infty} \mathbf{IM}\{B_{m,n,p-m,q-n}\} \quad (14)$$

where $\mathbf{IM}\{ \}$ indicates the imaginary part. Similar evolution equations for the energy spectrum of unidirectional waves are given by Agnon *et al.* [1993] and Eldeberky and Battjes [1995].

An evolution equation for the bispectrum is obtained in a similar fashion by taking the x derivative of (13)

$$\begin{aligned} \frac{dB_{m,n,p-m,q-n}}{dx} = & \mathbf{E} \left\{ \frac{dA_{m,n}}{dx} A_{p-m,q-n} A_{-p,-q} \right\} \\ & + \mathbf{E} \left\{ A_{m,n} \frac{dA_{p-m,q-n}}{dx} A_{-p,-q} \right\} \\ & + \mathbf{E} \left\{ A_{m,n} A_{p-m,q-n} \frac{dA_{-p,-q}}{dx} \right\} \end{aligned} \quad (15)$$

and substituting (11)

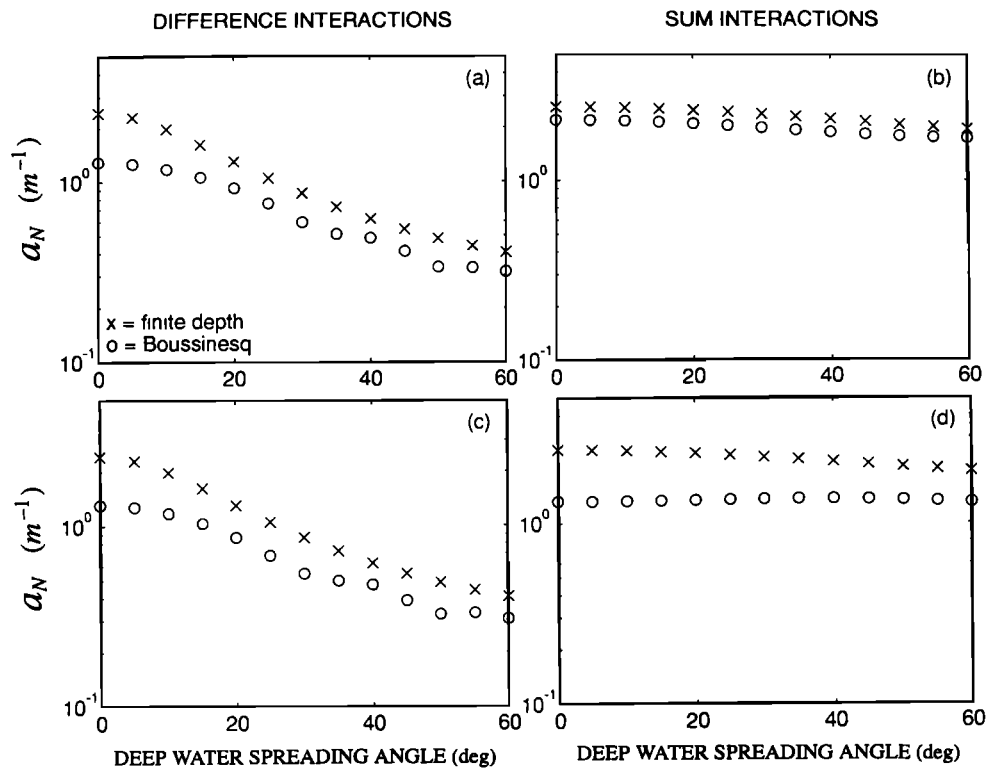


Figure 5. Directional dependence of the secondary wave response in 4 m depth for a pair of primary waves with frequencies 0.08 and 0.12 Hz on a beach with slope 0.01. Figures 5a and 5b and Figures 5c and 5d show results for deep water primary wave amplitudes of 0.1 and 0.4 m, respectively. (Same format as Figure 4)

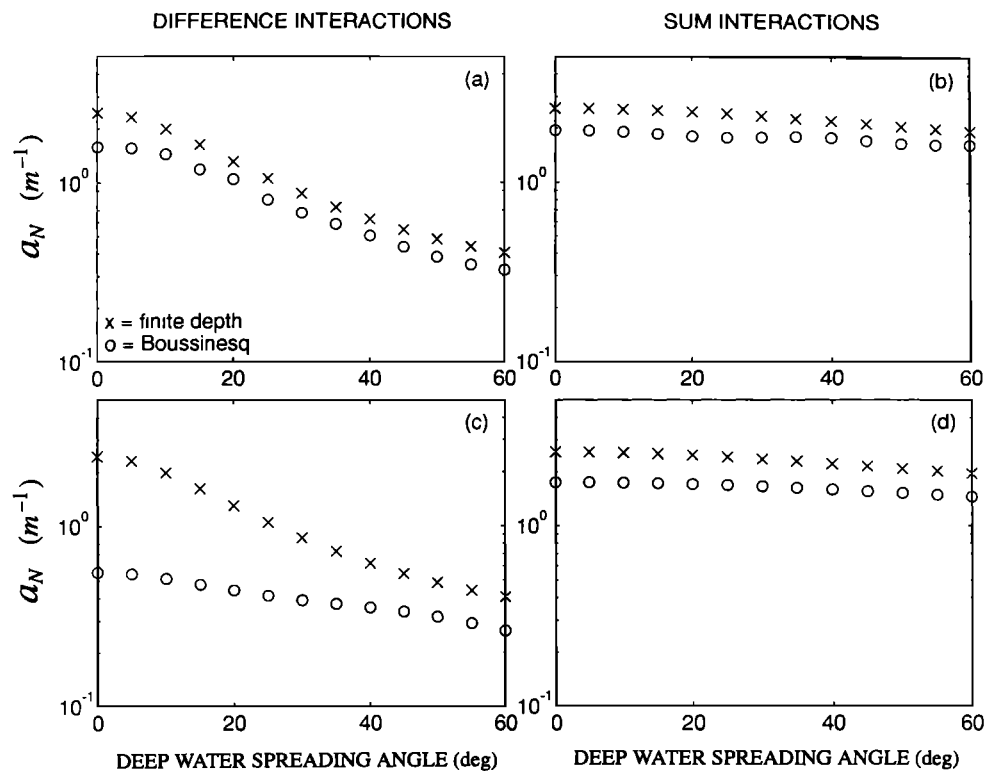


Figure 6. Directional dependence of the secondary wave response in 4 m depth for a pair of primary waves with frequencies 0.08 and 0.12 Hz on beaches with slope 0.003 (Figures 6a and 6b) and 0.03 (Figures 6c and 6d). The deep water amplitudes of both primary waves are 0.2 m. (Same format as Figure 4)

$$\begin{aligned} \frac{dB_{m,n,p-m,q-n}}{dx} = & \left\{ -\frac{3h_x}{4h} - i \left[\frac{h^{1/2}\omega_m\omega_{p-m}\omega_p}{2g^{3/2}} \right. \right. \\ & \left. \left. + \frac{(gh)^{1/2}(\omega_p l_n - \omega_m l_q)^2}{2\omega_m\omega_{p-m}\omega_p} \right] \right\} B_{m,n,p-m,q-n} \\ & - i \frac{3}{4h^{3/2}g^{1/2}} \sum_{r=-\infty}^{\infty} \sum_{s=-\infty}^{\infty} \{ \omega_m T_{r,s,m-r,n-s,p-m,q-n} \\ & + \omega_{p-m} T_{m,n,r,s,p-m-r,q-n-s} - \omega_p T_{m,n,p-m,q-n,r,s} \} \end{aligned} \quad (16)$$

with T the discrete trispectrum defined analogous to the bispectrum

$$T_{r,s,m,n,p-m-r,q-n-s} \equiv \mathbf{E}\{A_{r,s}A_{m,n}A_{p-m-r,q-n-s}A_{-p,-q}\} \quad (17)$$

In a weakly nonlinear wave field the trispectrum describes phase coupling between four wave components [Elgar *et al.*, 1995]. For example, if a primary wave component with frequency ω_{p-m} and alongshore wavenumber l_{q-n} engages in two nonlinear interactions: a sum interaction with an (ω_m, l_n) primary wave to excite an (ω_p, l_q) secondary wave and a difference interaction with an (ω_r, l_s) primary wave to excite an $(\omega_{p-m-r}, l_{q-n-s})$ secondary wave, then the four wave components $A_{r,s}, A_{m,n}, A_{p-m-r,q-n-s}$, and $A_{p,q}$ are phase locked and $T_{r,s,m,n,p-m-r,q-n-s}$ is nonzero. Alternatively, three primary wave components (ω_r, l_s) , (ω_m, l_n) , and $(\omega_{p-m-r}, l_{q-n-s})$ may drive an (ω_p, l_q) tertiary wave in a sum quartet interaction, also causing a nonzero value of $T_{r,s,m,n,p-m-r,q-n-s}$. In the limit of weak nonlinearity the contributions of a pair of triad interactions and a single quartet interaction to the trispectrum are formally of the same order, and thus a third-order theory is needed to describe the effects of phase coupling between four wave components. However, the trispectrum evolution equation (which can be derived in a similar fashion as (14) and (16)) depends on even higher-order nonlinearities. Approximate solutions for statistical properties of weakly nonlinear waves can be obtained only if a closure hypothesis is invoked.

4. Third-Order Closure

Since the Boussinesq equations used in the present study are truncated at second order in nonlinearity, a consistent closure approximation neglects the effects of nonlinear phase coupling between four wave components altogether so that the trispectrum reduces to the Gaussian expression

$$\begin{aligned} T_{r,s,m,n,p-m-r,q-n-s} = & E_{r,s}E_{m,n}\delta_{pm}\delta_{qn} + E_{m,n}E_{p,q}\delta_{rp}\delta_{sq} \\ & + E_{r,s}E_{p,q}\delta_{m(-r)}\delta_{n(-s)} \end{aligned} \quad (18)$$

where δ_{ij} is the Kronecker delta symbol. In this approximation, average products of two secondary and two primary wave amplitudes (and terms involving higher-order wave components, e.g., one tertiary and three primary waves) are neglected. Initially, these nonlinear quartet terms are small compared to the leading order terms (products of four primary components) kept in (18), but the cumulative effect of weak nonlinear triad interactions over large interaction distances may result in comparable amplitudes of primary and secondary waves. However, the trispectrum is an average over statistically independent realizations, and variations in biphases between different realizations (e.g., different incident wave amplitudes) will tend to

reduce the average products of primary and secondary wave amplitudes. Initially, when secondary wave amplitudes are relatively small (i.e., $U_r \ll 1$), phase coupling between primary and secondary waves is strong because in each realization, biphases are close to the finite depth theory values 0 (sum interactions, equation (6c)) or 180° (difference interactions, equations (6a) and (6b)). As secondary waves grow to appreciable amplitudes, the associated biphases evolve. In the Boussinesq approximation ($U_r = O(1)$), $O(1)$ changes in both wave amplitudes, and biphases occur over distances of $O[(a/h)^{-1}]$ wavelengths (equation (5) and Appendix A). The long-term evolution of a single wave triad (e.g., equation (5)) exhibits periodic recurrence cycles in which energy is transferred back and forth between the components [e.g., Armstrong *et al.*, 1962; Mei, 1983]. If a finite number of higher harmonics are included in the computations, these recurrence cycles become irregular [Bryant, 1973], and in a full spectrum of waves (e.g., equations (3a) and (3b)), energy exchanges between many different triads cause disordered amplitude evolution with a general spreading of energy to a broader range of frequencies and wavenumbers [Elgar *et al.*, 1990]. As wave amplitudes evolve through nonlinear energy exchanges, the associated biphases undergo comparably large changes and become increasingly sensitive to the initial amplitude configuration until they are effectively randomized (i.e., biphase values of independent realizations are approximately uniformly distributed between 0 and 360°). Hence, while the amplitudes of primary, secondary, and higher-order waves become comparable over large interaction distances, the initially strong nonlinear phase relationships are randomized, so that deviations from Gaussian statistics are expected to remain small.

Substitution of (18) into (16) yields the approximate bispectrum evolution equation

$$\begin{aligned} \frac{dB_{m,n,p-m,q-n}}{dx} = & \left\{ -\frac{3h_x}{4h} - i \left[\frac{h^{1/2}\omega_m\omega_{p-m}\omega_p}{2g^{3/2}} \right. \right. \\ & \left. \left. + \frac{(gh)^{1/2}(\omega_p l_n - \omega_m l_q)^2}{2\omega_m\omega_{p-m}\omega_p} \right] \right\} B_{m,n,p-m,q-n} - i \frac{3}{2h^{3/2}g^{1/2}} \\ & \cdot \{ \omega_m E_{p-m,q-n} E_{p,q} + \omega_{p-m} E_{m,n} E_{p,q} - \omega_p E_{m,n} E_{p-m,q-n} \} \end{aligned} \quad (19)$$

Note that the summation of the trispectrum in (16) is over all quartets that involve two of the components within the (m, n) , $(p-m, q-n)$, (p, q) triad, and thus (19) includes six nonvanishing trispectrum terms.

In the limit of infinitesimal separation between adjacent spectral components ($\Delta\omega, \Delta l \rightarrow 0$) a continuous density spectrum $E(\omega, l)$ and bispectrum $B(\omega', l', \omega - \omega', l - l')$ can be defined as

$$E_{p,q} \equiv E(\omega_p, l_q) \Delta\omega \Delta l \quad (20a)$$

$$B_{m,n,p-m,q-n} \equiv B(\omega_m, l_n, \omega_{p-m}, l_{q-n}) \Delta\omega^2 \Delta l^2 \quad (20b)$$

such that the integrals over all frequencies and alongshore wavenumbers yield the mean square and the mean cube of η (equations (7), (9), (13), (20a), and (20b))

$$\mathbf{E}\{\eta^2\} = \int_{-\infty}^{\infty} d\omega \int_{-\infty}^{\infty} dl E(\omega, l) \quad (21a)$$

$$\mathbf{E}\{\eta^3\} = \int_{-\infty}^{\infty} d\omega \int_{-\infty}^{\infty} dl \int_{-\infty}^{\infty} d\omega' \int_{-\infty}^{\infty} dl' B(\omega', l', \omega - \omega', l - l') \quad (21b)$$

Substitution of (20a) and (20b) into (14) and (19) yields (in the limit $\Delta\omega, \Delta l \rightarrow 0$) the following evolution equations for $E(\omega, l)$ and $B(\omega', l', \omega - \omega', l - l')$

$$\frac{dE(\omega, l)}{dx} = -\frac{h_x}{2h} E(\omega, l) + \frac{3\omega}{2h^{3/2}g^{1/2}} \cdot \int_{-\infty}^{\infty} d\omega' \int_{-\infty}^{\infty} dl' \text{IM}\{B(\omega', l', \omega - \omega', l - l')\} \quad (22a)$$

$$\begin{aligned} \frac{dB(\omega', l', \omega - \omega', l - l')}{dx} = & \left\{ -\frac{3h_x}{4h} - i \left[\frac{h^{1/2}\omega'(\omega - \omega')\omega}{2g^{3/2}} + \frac{(gh)^{1/2}(\omega l' - \omega' l)^2}{2\omega'(\omega - \omega')\omega} \right] \right\} \\ & \cdot B(\omega', l', \omega - \omega', l - l') - i \frac{3}{2h^{3/2}g^{1/2}} \\ & \cdot \{ \omega' E(\omega - \omega', l - l') E(\omega, l) \\ & + (\omega - \omega') E(\omega', l') E(\omega, l) \\ & - \omega E(\omega', l') E(\omega - \omega', l - l') \} \quad (22b) \end{aligned}$$

The first term on the right-hand sides of (22a) and (22b) represents linear shoaling (changes in group speed) effects. Nonlinear transfers in the spectrum $E(\omega, l)$ are controlled by the imaginary part of the bispectrum. From (22a) and the symmetry relations

$$\begin{aligned} B(\omega', l', \omega - \omega', l - l') &= B(\omega', l', -\omega, -l) \\ &= B(\omega - \omega', l - l', -\omega, -l) \end{aligned}$$

it follows that energy is conserved within each triad (i.e., the variance $\mathbf{E}\{\eta^2\}$ is not affected by nonlinear interactions). The last three terms (quadratic products of E) in (22b) represent changes in the imaginary part of $B(\omega', l', \omega - \omega', l - l')$ owing to the three possible nonlinear interactions (one sum and two difference interactions) within the (ω', l') , $(\omega - \omega', l - l')$, (ω, l) triad. The second and third term on the right-hand side of (22b) represent the resonance detuning effects (i.e., changes in the phase of the bispectrum) of dispersion and directional spreading, respectively.

In the limit $h_x \rightarrow 0$, (22a) and (22b) have a simple steady solution

$$\begin{aligned} B(\omega', l', \omega - \omega', l - l') &= -\frac{3g}{h^2} \left[\omega'(\omega - \omega')\omega + \frac{g^2(\omega l' - \omega' l)^2}{\omega'(\omega - \omega')\omega} \right]^{-1} \\ & \cdot \{ \omega' E(\omega - \omega', l - l') E(\omega, l) \\ & + (\omega - \omega') E(\omega', l') E(\omega, l) \\ & - \omega E(\omega', l') E(\omega - \omega', l - l') \} \quad (23) \end{aligned}$$

which is identical to the asymptotic shallow water limit of finite depth theory for small-amplitude waves (equation (B9) in Appendix B in discrete form). Thus, in the limit of weak nonlinearity and small bottom slope the spectrum and bispectrum evolution equations (22a) and (22b) decouple (i.e., the bispectrum depends only on the local spectrum), and the Boussinesq solutions smoothly match the solutions of dispersive finite

depth theory. It is interesting to note that the bispectrum B vanishes when the spectrum E is flat (i.e., independent of ω and l), suggesting that the gradual broadening of wave spectra owing to nonlinear triad interactions is accompanied by complete randomization of biphases. This result is consistent with numerical flat bottom simulations by *Elgar et al.* [1990] (using a deterministic Boussinesq model) that show an initially narrow spectrum evolving to a broad, featureless spectrum with weak phase coupling. Evolution to a featureless spectrum is not commonly observed on natural beaches where waves typically break well before secondary wave amplitudes become comparable to the primary wave amplitudes.

The effects of nonlinear triad interactions on continuous wave spectra are illustrated in Figure 7 with numerical predictions of the shoaling evolution of unidirectional (i.e., $l = 0$) waves from 8 to 2 m depth over a plane beach with slope 0.01. The initial significant wave height in these computations is 0.8 m, and the spectral shapes are representative of remotely generated swell (Figure 7a) and locally generated seas (Figure 7b). Bispectra were initialized in 8 m depth with the local bispectrum-spectrum relationship (equations (B5) and (B7) in Appendix B) of finite depth theory. The coupled evolution equations (22a) and (22b) were then integrated numerically, yielding predictions of spectra and bispectra in shallower water [see *Norheim*, 1997].

The predicted evolution of a swell spectrum (Figure 7a, peak frequency 0.07 Hz) shows the familiar development of harmonic peaks at frequencies 0.14, 0.21, 0.28, and 0.35 Hz. Initially, energy is transferred from the primary peak to the second harmonic (0.14 Hz) peak in (0.07, 0.07, 0.14 Hz) sum triad interactions. As the 0.14 Hz harmonic energy levels increase, energy is transferred in (0.07, 0.14, 0.21 Hz) triads to the third harmonic (0.21 Hz) peak. The fourth harmonic (0.28 Hz) peak is driven by both (0.07, 0.21, 0.28 Hz) and (0.14, 0.14, 0.28 Hz) sum triad interactions. Thus energy cascades from the initial swell peak toward higher frequencies through multiple sum triad interactions. Energy is also transferred to low (infragravity) frequencies (note the 0.01 Hz peak) through difference triad interactions involving pairs of primary swell (frequencies ≈ 0.07 Hz) components. As the harmonic and infragravity peaks in the spectrum grow (at the expense of the primary swell peak), triad interactions involving many different frequencies gradually fill the valleys between the peaks, and the spectrum evolves to a broad, almost featureless shape in 2 m depth.

The predicted evolution of a sea spectrum (Figure 7b, peak frequency 0.1 Hz) shows comparable nonlinear energy transfers to higher (sum triad interactions) and lower (difference triad interactions) frequencies. However, in this broader spectrum a wider range of frequencies participates in the interactions, causing a gradual broadening of the spectrum rather than the development of distinct harmonic peaks characteristic of swell spectra (Figure 7a). Although the shoaling evolution of the swell and sea spectra differ initially (compare the predictions in 6 and 4 m depth), the principal effect of nonlinear interactions is to distribute energy equally across the spectrum. Hence, over long distances these different wave fields tend to evolve to rather similar broad, almost featureless spectra (compare the predictions in 2 m depth). A detailed discussion of wave spectrum and bispectrum evolution on beaches, including numerical examples for a range of beach profiles and incident wave conditions and comparisons of stochastic and determin-

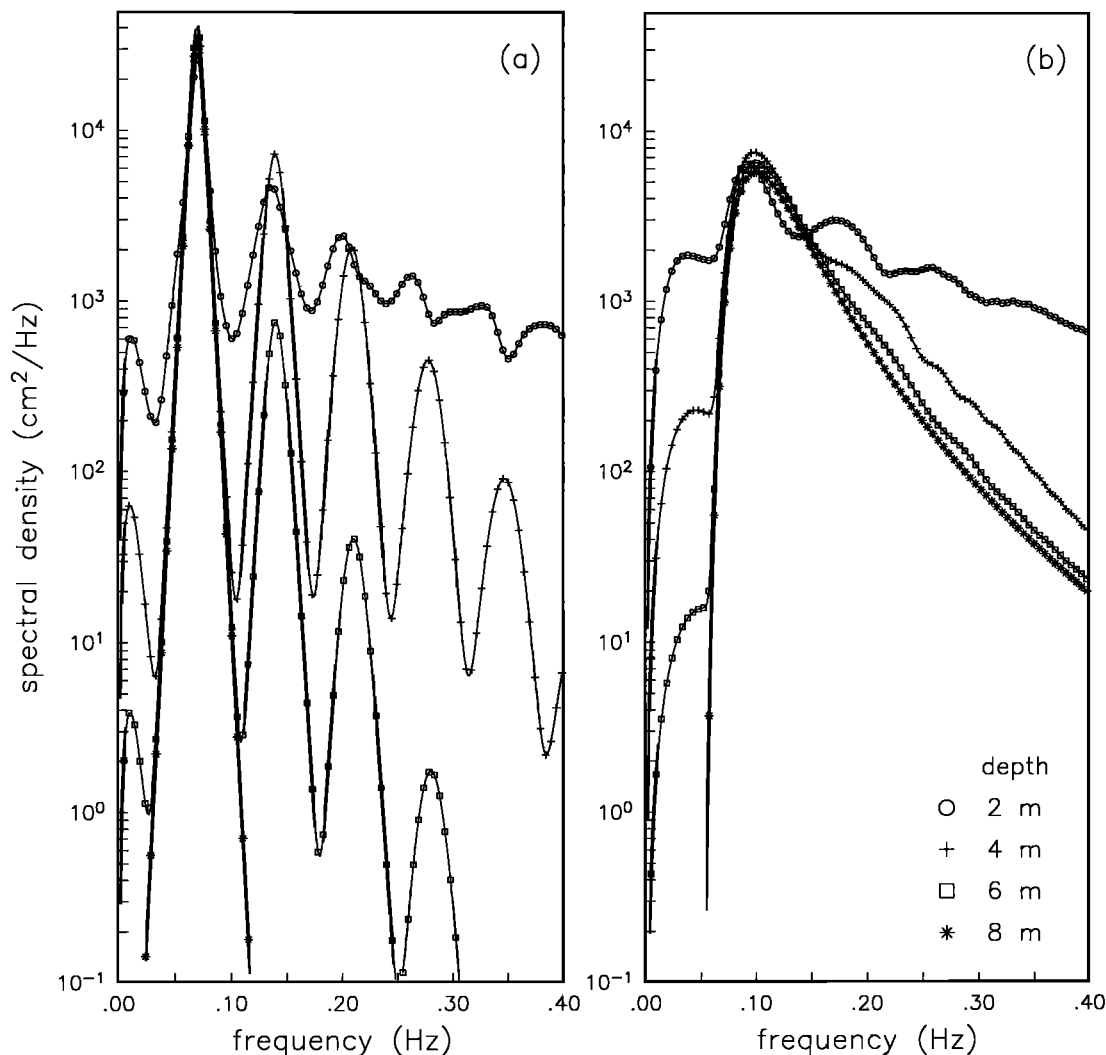


Figure 7. Example predictions of the nonlinear shoaling evolution of (a) a narrow swell and (b) a broad sea spectrum on a plane beach with slope 0.01. The initial significant wave height $[4(E\{\eta^2\})^{1/2}]$ in 8 m depth is 0.8 m, and the peak frequencies of the incident wave spectra are 0.07 Hz (Figure 7a) and 0.1 Hz (Figure 7b).

istic Boussinesq model predictions to field observations, is given by C. A. Norheim et al. (manuscript in preparation, 1997).

5. Summary and Discussion

Although wave transformation on beaches is generally well described by one-dimensional models, the directionality of waves is of crucial importance to a variety of nearshore processes including infragravity motions, longshore currents, and sediment transport. In this paper the shoaling of directionally spread waves is investigated using Boussinesq-type equations for weakly nonlinear, weakly dispersive waves in varying depth [Peregrine, 1967]. A gently sloping beach with straight and parallel depth contours is assumed on which wave incidence angles are reduced by refraction and reflection is neglected. In this approximation the effects of dispersion and directional spreading are of the same order, and near-resonant nonlinear interactions occur between any pair of wave components incident from deep water.

Boussinesq theory predictions of the shoaling evolution of a single triad of three wave components on a plane beach are

compared to predictions of dispersive, second-order finite depth theory [Hasselmann, 1962] for a typical range of beach slopes, swell amplitudes, frequencies, and propagation directions (Figures 2–6). In these simulations, two primary swell components arriving from deep water force a secondary wave on the beach, and interactions with any other components are neglected. The dependencies of the predicted secondary wave response on the directional spreading angle of the primary waves are in good agreement. Whereas the sum frequency response is only slightly reduced for large spreading angles, difference interactions are sensitive to the primary wave directions with typical reductions in secondary wave amplitudes of a factor of 3–10 when the primary wave spreading angle in deep water is increased from 0 to 60°.

An alternative stochastic formulation of Boussinesq theory is presented that describes the shoaling transformation of continuous spectra of random, directionally spread waves on a beach with straight and parallel depth contours. Under the closure hypothesis of weakly non-Gaussian statistics (neglecting phase coupling between quartets of wave components) a

coupled set of evolution equations is derived for the frequency alongshore wavenumber spectrum and bispectrum (equations (22a) and (22b)).

In the limit of weak nonlinearity and small bottom slope, steady solutions of Boussinesq theory (both the deterministic and stochastic formulations) are shown to match exactly steady bound wave solutions of finite depth theory. Although the theories are based on different assumptions, they describe, in essence, the same phenomenon of secondary wave generation in triad interactions. In dispersive finite depth theory the triad interactions are nonresonant. Two primary waves obeying the dispersion relation force a secondary (bound) wave that does not obey the dispersion relation. The amplitude of this bound wave is determined by the local amplitudes of the primary waves. As the primary waves gradually shoal, the mismatch of the bound wave from the dispersion relation is reduced, resulting in an amplification of the bound wave. Finite depth theory breaks down in shallow water where the interaction is resonant (i.e., the bound wave obeys the dispersion relation) and the predicted bound wave amplitude is infinite. Weakly dispersive Boussinesq theory, on the other hand, describes the continuous transfer of energy from two primary wave components to a freely propagating secondary wave component. The small mismatch of the triad interaction from resonance is incorporated by allowing for a slow modulation of wave amplitudes and phases that is equivalent to a small deviation of the wave frequency and wavenumber from the dispersion relation. Boussinesq theory breaks down in deep water where $O(1)$ deviations from the dispersion relation cause rapid variations in wave amplitudes and phases. The two theories overlap for small-amplitude waves shoaling on a gently sloping beach and thus describe a smooth transition of secondary waves from small nonresonantly forced bound waves in deep water to resonantly forced free waves in shallow water.

Although, formally, dispersive finite depth theory and weakly dispersive Boussinesq theory match only in the asymptotic limit of small wave amplitudes and beach slope, the simulations presented here indicate a reasonably smooth overlap region for commonly observed wave heights and beach slopes. These results are qualitatively consistent with field data. *Herbers et al.* [1992] compared velocity and pressure measurements in 6 m depth to finite depth theory predictions and found reasonable agreement for Ursell numbers (i.e., the predicted ratio of secondary to primary wave amplitudes) as large as 0.2. *Freilich and Guza* [1984] showed, for similar beach and wave conditions, that Boussinesq predictions initialized in 10 m depth ($\kappa h \approx 0.5$ with κ the wavenumber of the dominant waves) accurately reproduced the observed harmonic growth. Both finite depth and Boussinesq theories appear to be robust in the transition region from nonresonant to near-resonant triad interactions. In many applications, reasonably accurate predictions of wave shoaling evolution from deep to shallow water may be obtained by switching from finite depth theory to Boussinesq theory somewhere in the depth region where both U_r and κh are sufficiently small. However, in more extreme conditions, finite depth theory may break down (i.e., predict harmonics that are not small compared to the primary waves) well before κh is small; in which case, there is no overlap with Boussinesq theory. The shoaling process of extreme (e.g., hurricane-generated) swell or steep locally generated wind waves, with strong nonlinear evolution and breaking in intermediate water depths ($\kappa h = O(1)$), remains poorly understood.

Appendix A: Weakly Dispersive Boussinesq Theory

The equations of motion and the continuity equation can be written in nondimensionalized form (neglecting viscous effects):

$$\frac{\partial \mathbf{u}}{\partial t} + (\mathbf{u} \cdot \nabla) \mathbf{u} + w \frac{\partial \mathbf{u}}{\partial z} + \nabla p = 0 \quad (\text{A1a})$$

$$\frac{\partial w}{\partial t} + (\mathbf{u} \cdot \nabla) w + w \frac{\partial w}{\partial z} + \frac{\partial p}{\partial z} + 1 = 0 \quad (\text{A1b})$$

$$\nabla \cdot \mathbf{u} + \frac{\partial w}{\partial z} = 0 \quad (\text{A1c})$$

where t is time, ∇ denotes the two-dimensional gradient operator ($\partial/\partial x$, $\partial/\partial y$), \mathbf{u} is the vector (u , v) of the horizontal (x , y) velocity components, w is the vertical (z) velocity component, and p is pressure. The x axis points onshore; y points alongshore; and z points upward with $z = 0$ corresponding to the mean surface. The surface and bottom are defined by $z = \eta(x, y, t)$ and $z = -h(x)$ (Figure 1, alongshore depth variations are neglected). The variables in (A1) are normalized with the gravity g , the density of seawater ρ , and a representative water depth h_0 (Figure 1) [see also *Peregrine*, 1967]. The surface and bottom boundary conditions are given by

$$w = \frac{\partial \eta}{\partial t} + \mathbf{u} \cdot \nabla \eta \quad z = \eta \quad (\text{A2a})$$

$$p = 0 \quad z = \eta \quad (\text{A2b})$$

$$w = -u \frac{\partial h}{\partial x} \quad z = -h \quad (\text{A2c})$$

The variables η , u , v , w , and p are expanded in terms of the nonlinearity parameter ε , defined to be the ratio of wave amplitude to water depth, $\varepsilon \equiv a/h$. In shallow water, v and w are both $O(\kappa h)$ smaller than u , and thus the perturbation expansions of the scaled variables are given by

$$\eta = \varepsilon \eta_1 + \varepsilon^2 \eta_2 + \dots \quad (\text{A3a})$$

$$u = \varepsilon u_1 + \varepsilon^2 u_2 + \dots \quad (\text{A3b})$$

$$v = \sigma(\varepsilon v_1 + \varepsilon^2 v_2 + \dots) \quad (\text{A3c})$$

$$w = \sigma(\varepsilon w_1 + \varepsilon^2 w_2 + \dots) \quad (\text{A3d})$$

$$p = -z + \varepsilon p_1 + \varepsilon^2 p_2 + \dots \quad (\text{A3e})$$

where $\sigma \equiv \kappa h$ is the dispersion parameter. The independent variables are scaled

$$\frac{\partial}{\partial x} = \sigma \frac{\partial}{\partial x'} \quad (\text{A4a})$$

$$\frac{\partial}{\partial y} = \sigma^2 \frac{\partial}{\partial y'} \quad (\text{A4b})$$

$$\frac{\partial}{\partial z} = \frac{\partial}{\partial z'} \quad (\text{A4c})$$

$$\frac{\partial}{\partial t} = \sigma \frac{\partial}{\partial t'} \quad (\text{A4d})$$

so that the order of the terms appears explicitly when (A3) and (A4) are substituted into the governing equations [*Peregrine*,

1967]. Dispersion σ^2 and nonlinearity ε are assumed to be of the same order, and the water depth is taken to be a function $h(\bar{x})$ of the slow variable $\bar{x} = \varepsilon x'$

$$\frac{dh}{dx'} = \varepsilon \frac{dh}{d\bar{x}} \quad (\text{A5})$$

Substitution of (A3)–(A5) into the governing equations (A1a)–(A1c) using the boundary conditions (A2) and assuming irrotational flow yields the following relations for the first- and second-order flow variables [e.g., *Peregrine*, 1967]

$$p_1 = \eta_1 \quad (\text{A6a})$$

$$p_2 = \eta_2 + \left(z'h + \frac{z'^2}{2} \right) \frac{\partial^2 u_1}{\partial x' \partial t'} \quad (\text{A6b})$$

$$w_1 = -(h + z') \frac{\partial u_1}{\partial x'} \quad (\text{A6c})$$

$$u_2 = \bar{u}_2 - \left(\frac{h^2}{3} + z'h + \frac{z'^2}{2} \right) \frac{\partial^2 u_1}{\partial x'^2} \quad (\text{A6d})$$

$$v_2 = \bar{v}_2 - \left(\frac{h^2}{3} + z'h + \frac{z'^2}{2} \right) \frac{\partial^2 u_1}{\partial x' \partial y'} \quad (\text{A6e})$$

where u_1 and v_1 are independent of z' and \bar{u}_2 and \bar{v}_2 are the depth-averaged second-order flows. To $O(\varepsilon^2)$ these velocities can be expressed as gradients of velocity potential functions ϕ_1 and $\bar{\phi}_2$, and the momentum and (vertically integrated) continuity equations reduce to

$$\eta_{1x} + \phi_{1xt} + \varepsilon(\eta_{2x} + \bar{\phi}_{2xt} + \phi_{1x}\phi_{1xx} - \frac{1}{3}h^2\phi_{1xxx}) = O(\varepsilon^2) \quad (\text{A7a})$$

$$\eta_{1y} + \phi_{1yt} + \varepsilon(\eta_{2y} + \bar{\phi}_{2yt} + \phi_{1y}\phi_{1xy} - \frac{1}{3}h^2\phi_{1xyt}) = O(\varepsilon^2) \quad (\text{A7b})$$

$$\eta_{1t} + h\phi_{1xt} + \varepsilon[\eta_{2t} + h\bar{\phi}_{2xt} + h\phi_{1yy} + (\eta_1\phi_{1x})_x + \phi_{1x}h_{\bar{x}}] = O(\varepsilon^2) \quad (\text{A7c})$$

where subscripts t , x , and y indicate derivatives and the primes are dropped to simplify the notation.

The lowest-order wave field (η_1 , ϕ_1) is assumed to be a linear superposition of nearly plane, shoreward propagating waves [e.g., *Freilich and Guza*, 1984; *Kirby*, 1990]

$$\eta_1 = \sum_{p=-\infty}^{\infty} \sum_{q=-\infty}^{\infty} \frac{1}{2} a_{p,q}(\bar{x}) \exp \{i[\psi_{p,q}(x) + l_q y - \omega_p t]\} \quad (\text{A8a})$$

$$\phi_1 = \sum_{p=-\infty}^{\infty} \sum_{q=-\infty}^{\infty} \frac{1}{2i\omega_p} a_{p,q}(\bar{x}) \exp \{i[\psi_{p,q}(x) + l_q y - \omega_p t]\} \quad (\text{A8b})$$

where $\omega_p = p\Delta\omega$ and $l_q = q\Delta l$ are the (scaled) frequency and alongshore wavenumber, with $\Delta\omega$ and Δl the separation of adjacent bands in the Fourier representation. The amplitude $a_{p,q}$ is a slow function of x owing to shoaling (i.e., changes in the group speed) and nonlinear interactions. The phase function $\psi_{p,q}$ contains both fast and slow variations with x

$$\frac{d\psi_{p,q}(x)}{dx} = \frac{\omega_p}{h(\bar{x})^{1/2}} + \varepsilon T_{p,q}(\bar{x}) \quad (\text{A9})$$

The first term on the right-hand side of (A9) is the shallow water wavenumber, and $T_{p,q}$ incorporates the slow phase changes that result from weak dispersion, oblique propagation, and nonlinear interactions. The requirement that η_1 and ϕ_1 are real yields the symmetry relations

$$a_{p,q} = a_{-p,-q} \quad \psi_{p,q} = -\psi_{-p,-q} \quad T_{p,q} = -T_{-p,-q}$$

The governing equations (A7a)–(A7c) are cross differentiated to eliminate η_2 :

$$\nabla \left\{ \phi_{1tt} - h\phi_{1xx} + \varepsilon \left[\bar{\phi}_{2tt} - h\bar{\phi}_{2xx} + \frac{1}{2}(\phi_{1x}^2)_t - \frac{1}{3}h^2\phi_{1xxx} - h\phi_{1yy} - (\eta_1\phi_{1x})_x - h_{\bar{x}}\phi_{1x} \right] \right\} = O(\varepsilon^2) \quad (\text{A10})$$

Integration of (A10), setting the integration constant (an arbitrary function of time) equal to zero, yields

$$\phi_{1t} - h\phi_{1x} + \varepsilon \left[\bar{\phi}_{2t} - h\bar{\phi}_{2x} + \frac{1}{2}(\phi_{1x}^2)_t - \frac{1}{3}h^2\phi_{1xxx} - h\phi_{1yy} - (\eta_1\phi_{1x})_x - h_{\bar{x}}\phi_{1x} \right] = O(\varepsilon^2) \quad (\text{A11})$$

Substitution of the lowest-order wave field (equations (A8) and (A9)) into (A11) gives, after some algebraic manipulations,

$$\begin{aligned} \bar{\phi}_{2t} - h\bar{\phi}_{2x} = & \sum_{p=-\infty}^{\infty} \sum_{q=-\infty}^{\infty} \left\{ \frac{h_{\bar{x}}}{4h^{3/2}} a_{p,q} + h^{1/2} \frac{da_{p,q}}{d\bar{x}} \right. \\ & + i \left(h^{1/2} T_{p,q} - \frac{h\omega_p^3}{6} + \frac{hl_q^2}{2\omega_p} \right) a_{p,q} + i \frac{3\omega_p}{8h} \\ & \cdot \left. \sum_{m=-\infty}^{\infty} \sum_{n=-\infty}^{\infty} a_{m,n} a_{p-m,q-n} \exp [i(\psi_{m,n} + \psi_{p-m,q-n} - \psi_{p,q})] \right\} \\ & \cdot \exp [i(\psi_{p,q} + l_q y - \omega_p t)] + O(\varepsilon) \quad (\text{A12}) \end{aligned}$$

Resonant growth of $\bar{\phi}_2$ (which would upset the perturbation expansion (equation (A3))) is prevented by the solubility constraint that the right-hand side forcing terms in (A12) do not contain any free wave solutions of the general form $F(x/h^{1/2} \pm t)$. Since all these terms obey to $O(\varepsilon)$ the shallow water dispersion relation (equation (A9)), it follows that the right-hand side of (A12) must vanish. Collecting the real and imaginary parts of like frequencies and alongshore wavenumbers yields a coupled set of evolution equations for the amplitudes and phases of the lowest-order waves:

$$\begin{aligned} \frac{da_{p,q}}{d\bar{x}} = & -\frac{h_{\bar{x}}}{4h} a_{p,q} + \frac{3\omega_p}{8h^{3/2}} \\ & \cdot \sum_{m=-\infty}^{\infty} \sum_{n=-\infty}^{\infty} a_{m,n} a_{p-m,q-n} \sin (\psi_{m,n} + \psi_{p-m,q-n} - \psi_{p,q}) \quad (\text{A13a}) \end{aligned}$$

$$\begin{aligned} T_{p,q} = & \frac{h^{1/2}\omega_p^3}{6} - \frac{h^{1/2}l_q^2}{2\omega_p} - \frac{3\omega_p}{8h^{3/2}a_{p,q}} \\ & \cdot \sum_{m=-\infty}^{\infty} \sum_{n=-\infty}^{\infty} a_{m,n} a_{p-m,q-n} \cos (\psi_{m,n} + \psi_{p-m,q-n} - \psi_{p,q}) \quad (\text{A13b}) \end{aligned}$$

Appendix B: Dispersive Finite Depth Theory

In second-order finite depth theory the surface elevation function η is given by

$$\eta(x, y, t) = \eta_1(x, y, t) + \eta_2(x, y, t) \quad (\text{B1})$$

where η_1 is the wind-generated primary wave field and η_2 contains the associated secondary bound waves. The primary wave field is assumed to be a linear superposition of statistically independent, nearly plane wave components propagating over a gently sloping seabed with straight and parallel depth contours

$$\eta_1(x, y, t) = \sum_{p=-\infty}^{\infty} \sum_{q=-\infty}^{\infty} \Xi_{p,q}(x) \exp [i(l_y y - \omega_p t)] \quad (\text{B2})$$

where the complex amplitude function $\Xi_{p,q}(x)$ is given by the linear shoaling refraction relation [e.g., *Kinsman, 1965*]

$$\Xi_{p,q}(x) = \Xi_{p,q}(0) \cdot \left[\frac{c_{g_p}(0)k_{p,q}(0)\kappa_p(x)}{c_{g_p}(x)k_{p,q}(x)\kappa_p(0)} \right]^{1/2} \exp \left[i \int_0^x dx k_{p,q}(x) \right] \quad (\text{B3})$$

The wavenumber magnitude $\kappa_p = (k_{p,q}^2 + l_q^2)^{1/2}$ obeys the linear dispersion relation $\omega_p^2 = g\kappa_p \tanh(\kappa_p h)$, and the group speed is given by $c_{g_p} = (\omega_p/\kappa_p)[1/2 + \kappa_p h/\sinh(2\kappa_p h)]$. The condition that η_1 is real implies that $\Xi_{-p,-q}(x)$ is the complex conjugate of $\Xi_{p,q}(x)$. The cross-shore wavenumber component $k_{p,q}$ is positive for $p > 0$ (i.e., waves propagate shoreward, Figure 1) and $k_{-p,-q}(x) = -k_{p,q}(x)$.

The corresponding secondary wave field is given by [*Hasselmann, 1962, equation (4.2)*]

$$\eta_2(x, y, t) = \sum_{p=-\infty}^{\infty} \sum_{q=-\infty}^{\infty} \sum_{m=-\infty}^{\infty} \sum_{n=-\infty}^{\infty} D(\omega_m, l_n, \omega_{p-m}, l_{q-n}; x) \cdot \Xi_{m,n}(x) \Xi_{p-m,q-n}(x) \exp [i(l_y y - \omega_p t)] \quad (\text{B4})$$

where D is the nonlinear coupling coefficient

$$D(\omega_m, l_n, \omega_{p-m}, l_{q-n}) = \frac{\omega_p^2}{g|\mathbf{k}_{m,n} + \mathbf{k}_{p-m,q-n}| \tanh(|\mathbf{k}_{m,n} + \mathbf{k}_{p-m,q-n}|h) - \omega_p^2} \cdot \left\{ \frac{\omega_m \omega_{p-m}}{g} - \frac{g\mathbf{k}_{m,n} \cdot \mathbf{k}_{p-m,q-n}}{\omega_m \omega_{p-m}} - \frac{g}{2\omega_p} \left[\frac{\kappa_m^2}{\omega_m \cosh^2(\kappa_m h)} + \frac{\kappa_{p-m}^2}{\omega_{p-m} \cosh^2(\kappa_{p-m} h)} \right] \right\} + \frac{\omega_m^2 + \omega_m \omega_{p-m} + \omega_{p-m}^2}{2g} - \frac{g\mathbf{k}_{m,n} \cdot \mathbf{k}_{p-m,q-n}}{2\omega_m \omega_{p-m}} \quad (\text{B5})$$

with $\mathbf{k}_{i,j} = (k_{i,j}, l_j)$ the vector wavenumber of primary wave component ω_i, l_j .

The combined wave field (equation (B1)) can be expressed in the general Fourier representation (7) with the amplitude function $A_{p,q}(x)$ given by

$$A_{p,q} = \Xi_{p,q} + \sum_{m=-\infty}^{\infty} \sum_{n=-\infty}^{\infty} D(\omega_m, l_n, \omega_{p-m}, l_{q-n}) \Xi_{m,n} \Xi_{p-m,q-n} \quad (\text{B6})$$

Substitution of (B6) into (9) and (13) yields a (lowest-order) relationship between the spectrum and bispectrum [*Hasselmann et al., 1963*]:

$$B_{m,n,p-m,q-n} = 2\{D(\omega_m, l_n, \omega_{p-m}, l_{q-n})E_{m,n}E_{p-m,q-n} + D(\omega_m, l_n, -\omega_p, -l_q)E_{m,n}E_{p,q} + D(\omega_{p-m}, l_{q-n}, -\omega_p, -l_q)E_{p-m,q-n}E_{p,q}\} \quad (\text{B7})$$

The asymptotic shallow water approximation of the bispectrum is obtained by expanding the coupling coefficient D (equation (B5)) for small κh [*Herbers et al., 1992, 1995*]

$$D(\omega_m, l_n, \omega_{p-m}, l_{q-n}) = \frac{3g}{2\omega_m \omega_{p-m} h^2} \cdot \left[1 + \frac{g^2}{\omega_p^2} \left(\frac{l_n}{\omega_m} - \frac{l_{q-n}}{\omega_{p-m}} \right)^2 \right]^{-1} \quad \kappa h \ll 1 \quad (\text{B8})$$

Substitution of (B8) into (B7) yields

$$B_{m,n,p-m,q-n} = -\frac{3g}{h^2} \left[\omega_m \omega_{p-m} \omega_p + \frac{g^2(\omega_p l_n - \omega_m l_q)^2}{\omega_m \omega_{p-m} \omega_p} \right]^{-1} \cdot \{\omega_m E_{p-m,q-n} E_{p,q} + \omega_{p-m} E_{m,n} E_{p,q} - \omega_p E_{m,n} E_{p-m,q-n}\} \quad \kappa h \ll 1 \quad (\text{B9})$$

Acknowledgments. This research was supported by the Office of Naval Research (Coastal Dynamics Program and the Nonlinear Ocean Waves Accelerated Research Initiative). C. A. Norheim developed the code for numerical integration of stochastic shoaling evolution equations. We thank R. T. Guza, M. H. Freilich, and S. Elgar for many helpful discussions and the anonymous reviewers for useful suggestions.

References

- Abreu, M., A. Larraza, and E. Thornton, Nonlinear transformation of directional wave spectra in shallow water, *J. Geophys. Res.*, 97, 15,579–15,589, 1992.
- Agnon, Y., A. Sheremet, J. Gonsalves, and M. Stiassnie, Nonlinear evolution of a unidirectional shoaling wave field, *Coastal Eng.*, 20, 29–58, 1993.
- Armstrong, J. A., N. Bloembergen, J. Ducuing, and P. S. Persham, Interactions between light waves in a nonlinear dielectric, *Phys. Rev.*, 127, 1918–1939, 1962.
- Bryant, P. J., Periodic waves in shallow water, *J. Fluid Mech.*, 59, 625–644, 1973.
- Chen, Y., and P. L.-F. Liu, Modified Boussinesq equations and associated parabolic models for water wave propagation, *J. Fluid Mech.*, 288, 351–381, 1995.
- Eldeberky, Y., and J. A. Battjes, Parameterisation of triad interactions in wave energy models, paper presented at Coastal Dynamics '95, Am. Soc. of Civ. Eng., Gdansk, Poland, 1995.
- Elgar, S., and R. T. Guza, Shoaling gravity waves: Comparisons between field observations, linear theory, and a nonlinear model, *J. Fluid Mech.*, 158, 47–70, 1985a.
- Elgar, S., and R. T. Guza, Observations of bispectra of shoaling surface gravity waves, *J. Fluid Mech.*, 161, 425–448, 1985b.
- Elgar, S., M. H. Freilich, and R. T. Guza, Recurrence in truncated Boussinesq models for nonlinear waves in shallow water, *J. Geophys. Res.*, 95, 11,547–11,556, 1990.
- Elgar, S., R. T. Guza, and M. H. Freilich, Observations of nonlinear interactions in directionally spread shoaling surface gravity waves, *J. Geophys. Res.*, 98, 20,299–20,305, 1993.
- Elgar, S., T. H. C. Herbers, V. Chandran, and R. T. Guza, Higher-order spectral analysis of nonlinear ocean surface gravity waves, *J. Geophys. Res.*, 100, 4977–4983, 1995.
- Flick, R. E., R. T. Guza, and D. L. Inman, Elevation and velocity

- measurements of laboratory shoaling waves, *J. Geophys. Res.*, *86*, 4149–4160, 1981.
- Freilich, M. H., and R. T. Guza, Nonlinear effects on shoaling surface gravity waves. *Philos. Trans. R. Soc. London*, *A311*, 1–41, 1984.
- Hasselmann, K., On the non-linear energy transfer in a gravity-wave spectrum, 1, General theory, *J. Fluid Mech.*, *12*, 481–500, 1962.
- Hasselmann, K., W. Munk, and G. MacDonald, Bispectra of ocean waves, in *Times Series Analysis*, edited by M. Rosenblatt, pp. 125–139, John Wiley, New York, 1963.
- Herbers, T. H. C., and R. T. Guza, Nonlinear wave interactions and high-frequency seafloor pressure, *J. Geophys. Res.*, *99*, 10,035–10,048, 1994.
- Herbers, T. H. C., R. L. Lowe, and R. T. Guza, Field observations of orbital velocities and pressure in weakly nonlinear surface gravity waves, *J. Fluid Mech.*, *245*, 413–435, 1992.
- Herbers, T. H. C., S. Elgar, and R. T. Guza, Infragravity-frequency (0.005–0.05 Hz) motions on the shelf, I, Forced waves, *J. Phys. Oceanogr.*, *24*, 917–927, 1994.
- Herbers, T. H. C., S. Elgar, and R. T. Guza, Generation and propagation of infragravity waves, *J. Geophys. Res.*, *100*, 24,863–24,872, 1995.
- Kaihatu, J. M., and J. T. Kirby, Spectral evolution of finite amplitude dispersive waves in shallow water, paper presented at 23rd International Conference on Coastal Engineering, Am. Soc. of Civ. Eng., Venice, Italy, 1992.
- Kaihatu, J. M., and J. T. Kirby, Nonlinear transformation of waves in finite water depth, *Phys. Fluids*, *7*, 1903–1914, 1995.
- Kinsman, B., *Wind Waves: Their Generation and Propagation on the Ocean Surface*. 676 pp. Prentice-Hall, Englewood Cliffs, N. J., 1965.
- Kirby, J. T., Modeling shoaling directional wave spectra in shallow water, paper presented at 22nd International Conference on Coastal Engineering, Am. Soc. of Civ. Eng., Delft, Netherlands, 1990.
- Liu, P. L.-F., S. B. Yoon, and J. T. Kirby, Nonlinear refraction-diffraction of waves in shallow water, *J. Fluid Mech.*, *153*, 185–201, 1985.
- Madsen, P. A., and O. R. Sørensen, Bound waves and triad interactions in shallow water, *Ocean Eng.*, *15*, 371–388, 1993.
- Madsen, P. A., R. Murray, and O. R. Sørensen, A new form of the Boussinesq equations with improved linear dispersion characteristics, *Coastal Eng.*, *15*, 371–388, 1991.
- Mei, C. C., *The Applied Dynamics of Ocean Surface Waves*, 740 pp., Wiley-Interscience, New York, 1983.
- Newell, A. C., and P. J. Aucoin, Semidispersive wave systems, *J. Fluid Mech.*, *49*, 593–609, 1971.
- Norheim, C. A., A stochastic model for shoaling waves, M. S. thesis, 47 pp., Naval Postgrad. Sch., Monterey, Calif., 1997.
- Nwogu, O., Alternative form of Boussinesq equations for nearshore wave propagation, *J. Waterw. Port Coastal Ocean Div. Am. Soc. Civ. Eng.*, *119*, 618–638, 1993.
- Nwogu, O., Nonlinear evolution of directional wave spectra in shallow water, paper presented at 24th International Conference on Coastal Engineering, Am. Soc. of Civ. Eng., Kobe, Japan, 1994.
- Peregrine, D. H., Long waves on a beach, *J. Fluid Mech.*, *27*, 815–827, 1967.
- Phillips, O. M., On the dynamics of unsteady gravity waves of finite amplitude, I, The elementary interactions, *J. Fluid Mech.*, *9*, 193–217, 1960.
- Ursell, F., The long-wave paradox in the theory of gravity waves, *Proc. Cambridge Philos. Soc.*, *49*, 685–694, 1953.
- The Wave Model Development and Implementation (WAMDI) Group, The WAM model: A third generation ocean wave prediction model, *J. Phys. Oceanogr.*, *18*, 1775–1810, 1988.
- Wei, G., J. T. Kirby, S. T. Grilli, and R. Subramanya, A fully nonlinear Boussinesq model for surface waves, I, Highly nonlinear, unsteady waves, *J. Fluid Mech.*, *294*, 71–92, 1995.

M. C. Burton and T. H. C. Herbers, Department of Oceanography, Code OC/He, Naval Postgraduate School, Monterey, CA 93943-5122. (e-mail: herbers@oc.nps.navy.mil)

(Received May 10, 1996; revised May 7, 1997; accepted May 29, 1997.)